

# **DEVELOPMENT OF RARE EARTH DOPED TITANATE PHOSPHOR FOR w-LED APPLICATIONS**

A DISSERTATION

SUBMITTED IN PARTIAL FULFILLMENT OF THE REQUIREMENTS

FOR THE AWARD DEGREE

OF

MASTER OF SCIENCE

IN

**Physics**

Submitted by:

**Vedika Dubey**

**(2K22/MSCPHY/47)**

**Tannavi**

**(2K22/MSCPHY/43)**

Under the supervision of

**Dr. M. Jayasimhadri**



**DEPARTMENT OF APPLIED PHYSICS**

**DELHI TECHNOLOGICAL UNIVERSITY**

(Formerly Delhi College of Engineering)

Bawana Road, Delhi-110042

**June, 2024**

## CANDIDATES' DECLARATION

We **Vedika Dubey** (2K22/MSCPHY/47), **Tannavi** (2K22/MSCPHY/43) hereby certify that the work which is presented in the thesis entitled "***Development of Rare Earth Doped Titanate Phosphor for w-LED Applications***" in partial fulfillment of the requirements for the award of the **Degree of Master of Science in Physics**, submitted in the Department of Applied Physics, Delhi Technological University, Delhi, is an authentic record of our own work carried out during the period from July 2023 to June 2024 under the supervision of **Dr. M. Jayasimhadri**.

The matter presented in the thesis has not been submitted by me for the award of any other degree of this or any other Institute. The work has been communicated in peer reviewed Scopus indexed conference and journal with the following details:

**Title of the Paper (I):** Luminescent features of red emitting  $\text{Eu}^{3+}$  induced yttrium niobium titanate phosphor for photonic applications

**Author names (in the sequence as per research paper):** Tannavi, Vedika Dubey and M. Jayasimhadri

**Name of Conference:** Recent Advances in Functional Materials (RAFM-2024)

**Name of the Journal:** Springer Nature Proceedings of RAFM 2024 (Scopus Indexed)

**Conference Dates with venue:** 2024, March 14-16, Online

**Have you registered for the conferences:** Yes

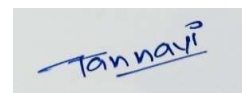
**Status of paper (Accepted/ Published/ Communicated):** Accepted

**Date of paper communication:** April, 2024

**Place:** Delhi



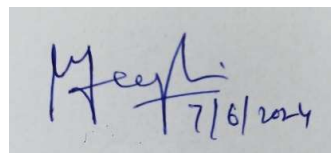
**Vedika Dubey**  
(2K22/MSCPHY/47)



**Tannavi**  
(2K22/MSCPHY/43)

**Date:** 07/06/2024

This is to certify that the students has incorporated all the corrections suggested by the examiners in the thesis and the statement made by the candidate is correct to the best of our knowledge.



**Signature of Supervisor**



# DELHI TECHNOLOGICAL UNIVERSITY

Formerly Delhi College of Engineering)  
Shahbad Daultapur, Main Bawana Road, Delhi-42

## CERTIFICATE BY THE SUPERVISOR

Certified that **Vedika Dubey** (2K22/MSCPHY/47), **Tannavi** (2K22/MSCPHY/43) has carried out their search work presented in this thesis entitled **“Development of Rare Earth Doped Titanate Phosphor for w-LED Applications”** for the award of **Master of Science in Physics** from Department of Applied Physics, Delhi Technological University, Delhi, under my supervision. The thesis embodies results of original work, and studies are carried out by the student herself and the contents of the thesis do not form the basis for the award of any other degree to the candidate or to anybody else from this or any other University/Institution.

**Place:** Delhi

Signature

**Dr. M. Jayasimhadri**

Assistant Professor

Department of Applied Physics

DTU, Delhi- 110042

**Date:** 07/06/2024

## **ACKNOWLEDGMENTS**

We would like to convey our heartfelt thanks to **Dr. M. Jayasimhadri**, Assistant Professor, Department of Applied Physics, Delhi Technological University, for allowing us to work under his supervision and for providing us with continual inspiration and unwavering support throughout the project. We'd like to take this occasion to thank our supervisor for his passionate assistance, knowledge, fantastic ideas, useful comments, and consistent support. We are appreciative of the continual assistance and convenience provided by all LMR lab members (Ph.D. scholars), especially Mr. Vikas Sangwan and Mr. Indrajeet Maurya at every stage of our study. Furthermore, we have been fortunate and thankful to our family and friends for their love, care, as they patiently extended all kinds of assistance to help us complete this duty.

**Vedika Dubey & Tannavi**

## ABSTRACT

Europium ( $\text{Eu}^{3+}$ ) induced yttrium niobium titanate ( $\text{YNbTiO}_6$ ) has been synthesized using a high-temperature solid state reaction synthesis route. The as-synthesised phosphor materials' structural, morphological and luminous characteristics have all been investigated via using characterization techniques, such as X-ray diffraction (X-RD), field emission scanning electron microscopy (FE-SEM) and photoluminescent (PLE and PL) studies, respectively. Pure and single-phase formation with orthorhombic structure of the synthesized  $\text{YNbTiO}_6$  (YNT) sample represents the irregular and agglomerated morphology, with non-uniform particle formation in a micron range. Upon being excited by UV (284 nm), NUV (394 nm) and blue (465 nm) lights, the synthesized YNT:  $\text{Eu}^{3+}$  phosphor emits several characteristics peaks of the  $\text{Eu}^{3+}$  ions and a dominant emission peak has been observed in the red region (612 nm). Moreover, the chromaticity coordinates were estimated for the synthesized 1.0 mol%  $\text{Eu}^{3+}$  induced YNT phosphor UV, NUV and blue excitations, respectively. Hence, the results mentioned above confirm that the synthesized YNT:  $\text{Eu}^{3+}$  phosphor could be useful as a red-emitting component for photonic applications.

## TABLE OF CONTENTS

<b>Title</b>	<b>i</b>
<b>Candidates' Declaration</b>	<b>ii</b>
<b>Certificate by the Supervisor</b>	<b>iii</b>
<b>Acknowledgments</b>	<b>iv</b>
<b>Abstract</b>	<b>v</b>
<b>Table of Contents</b>	<b>vi</b>
<b>List of Figures</b>	<b>viii</b>
<b>List of Abbreviations</b>	<b>x</b>
<b>Chapter 1: INTRODUCTION</b>	<b>1-12</b>
1.1. History	1
1.2. Luminescence	2
1.2.1. Classification Of Luminescence	2
1.2.2. Photoluminescence (PL)	3
1.2.2.1. Fluorescence And Phosphorescence	3
1.2.2.2. Photoluminescence Process	4
1.3. Rare Earth Ions/Lanthanides	5
1.3.1. Unique Features of Rare Earth Ions	7
1.4. Phosphor And Luminescence Mechanism	7
1.5. Application: White Light Emitting Diodes (w-LEDs)	8
1.5.1. Colorimetry Properties	10
1.6. Motivation & Objectives	11
<b>Chapter 2: SYNTHESIS AND EXPERIMENTAL PROCEDURE</b>	<b>13-19</b>
2.1. Synthesis Methods	13
2.1.1. Solid State Reaction (SSR) Method	13
2.1.2. Sol-Gel Method	14
2.1.3. Hydrothermal Method	15
2.1.4. Molten Salt Synthesis	16

2.1.5. Co-Precipitation Method	16
2.2. Synthesis of Phosphor Material	17
2.2.1. Selection of Host Material	17
2.2.2. Selection of Synthesis Route: SSR Method	18
2.2.3. Sample Preparation	18
2.2.4. Analysis of Sample	19
<b>Chapter 3: CHARACTERIZATION TECHNIQUES</b>	<b>20-23</b>
0.1. Characterization Techniques	20
0.1.1. X-Ray Diffraction (X-RD)	20
0.1.1.1. Joint Committee on Powder Diffraction Standards (JCPDS)	21
0.1.2. Field Emission Scanning Electron Microscopy (FE-SEM)	21
0.1.3. Photoluminescence (PL) Spectroscopy	22
<b>Chapter 4: RESULTS AND DISCUSSION</b>	<b>24-30</b>
4.1. Europium (Eu <sup>3+</sup> ) doped Yttrium Niobium Titanate (YNT) Phosphor	24
4.1.1. Structural Studies	24
4.1.2. Morphological Studies	25
4.1.3. Photoluminescence Studies	26
4.1.4. Colorimetric Studies	29
<b>CHAPTER 5: CONCLUSIONS AND FUTURE SCOPE OF WORK</b>	<b>31-32</b>
5.1. Conclusions	31
5.2. Future Scope of Work	32
<b>REFERENCES</b>	<b>33-36</b>
<b>CONFERENCE PROOF</b>	<b>37-38</b>
<b>I. CONFERENCE ACCEPTANCE PROOF</b>	<b>37</b>
<b>II. PUBLICATION ACCEPTANCE PROOF</b>	<b>37</b>
<b>III. PROOF OF SCOPUS INDEXING</b>	<b>38</b>
<b>PLAGIARISM REPORT</b>	<b>39</b>

## LIST OF FIGURES

<b>Fig. 1.1.</b>	Examples of luminescence	<b>1</b>
<b>Fig. 1.2.</b>	Types of luminescence based on different excitation sources and its duration	<b>2</b>
<b>Fig. 1.3.</b>	Jablonski diagram for fluorescence and phosphorescence	<b>4</b>
<b>Fig. 1.4.</b>	PL process (a) absorption, (b) excitation, (c) non-radiative relaxation, and (d) emission	<b>5</b>
<b>Fig. 1.5.</b>	Rare earth ions with their electronic configurations and oxidation state	<b>6</b>
<b>Fig. 1.6.</b>	(a) Direct absorption via activator, and (b) energy transfer (ET) by host or sensitizer to activator	<b>8</b>
<b>Fig. 1.7.</b>	Different approaches for white light generation via LEDs	<b>9</b>
<b>Fig. 1.8.</b>	CCT scale	<b>10</b>
<b>Fig. 2.1.</b>	Steps involved in solid state reaction method	<b>13</b>
<b>Fig. 2.2.</b>	Steps involved in sol-gel process of material synthesis	<b>14</b>
<b>Fig. 2.3.</b>	Steps involved in molten salt synthesis	<b>16</b>
<b>Fig. 2.4.</b>	Crystal structure of euxenite type $\text{YNbTiO}_6$	<b>17</b>
<b>Fig. 2.5.</b>	Steps for synthesis of $\text{YNT: xEu}^{3+}$ ( $x= 1.0$ mol%) phosphor via SSR method	<b>19</b>
<b>Fig. 3.1.</b>	X-ray diffraction machine	<b>20</b>
<b>Fig. 3.2.</b>	Bragg's Law	<b>20</b>
<b>Fig. 3.3.</b>	FE-SEM (Zeiss GeminiSEM 500)	<b>22</b>
<b>Fig. 3.4.</b>	PL (JASCO-8300FL) Spectrophotometer	<b>22</b>
<b>Fig. 4.1.</b>	Diffraction patterns of YNT host lattice & $\text{YNT: 1.0 mol\% Eu}^{3+}$ phosphor	<b>24</b>
<b>Fig. 4.2.</b>	FE-SEM micrograph for YNT host	<b>25</b>
<b>Fig. 4.3.</b>	PLE spectrum of the $\text{YNT: 1.0 mol\% Eu}^{3+}$ phosphor under $\lambda_{em}=612$ nm (Insert represents the PLE spectrum in the 340 to 480 nm range)	<b>26</b>



<b>Fig. 4.4.</b>	PL spectrum of the YNT: 1.0 mol% Eu <sup>3+</sup> phosphor under $\lambda_{exc}= 280$ nm	<b>27</b>
<b>Fig. 4.5.</b>	PL spectrum of YNT: 1.0 mol% Eu <sup>3+</sup> phosphor under $\lambda_{exc}= 394$ and 465 nm	<b>28</b>
<b>Fig. 4.6.</b>	Comparison of emission intensity at different excitation wavelengths of the YNT: 1.0 mol% Eu <sup>3+</sup> phosphor	<b>29</b>
<b>Fig. 4.7.</b>	CIE chromaticity coordinates for the synthesized YNT: 1.0 mol% Eu <sup>3+</sup> phosphor under UV, NUV and blue light	<b>30</b>

## **LIST OF ABBREVIATIONS**

RE	Rare Earth
UV	Ultraviolet
NUV	Near Ultraviolet
LED	Light Emitting Diode
w-LED	White Light Emitting Diode
SSL	Solid State Lighting
pc w-LED	Phosphor Converted White Light Emitting Diode
CRI	Color Rendering Index
CCT	Correlated Color Temperature
CIE	Commission Internationale de l'Éclairage
PL	Photoluminescence
YNT	Yttrium Niobium Titanate
SSR	Solid State Reaction
MSS	Molten Salt Synthesis
XRD	X-Ray Diffraction
JCPDS	Joint Committee on Powder Diffraction Standards
ICDD	International Centre for Diffraction Data
FE-SEM	Field Emission Scanning Electron Microscopy

## CHAPTER 1: INTRODUCTION

### 1.1. History

The term luminescence is derived from the Latin word, 'Lumen' meaning 'light' and materials exhibiting the phenomenon of luminescence were known as 'Luminescent materials' or 'Phosphors'. The year 1603, marks the beginning of modern luminescent material. Vincenzo Cascariolo, an Italian shoemaker and alchemist used mineral barite ( $\text{BaSO}_4$ ), to create gold. After heating the mineral, he did not obtained gold, but instead a persistent luminescent material. BaS is the first sulphide phosphor ever synthesised and is also known as Bologna stone. Vincenzo Cascariolo is credited with coining the term "phosphor" for the first time in the 17<sup>th</sup> century. Later in 1888, When Wiedemann classified luminescence into various kinds, depending on their source of excitation. In the 20<sup>th</sup> century, Lenard and co-researchers made an important discovery that, transition metal or rare earth ions could be added to produce phosphor at higher temperature. Since then, significant advancement has been made in phosphor technologies [1].



*Fig. 1.1. Examples of luminescence*

## 1.2. Luminescence

Light is a form of energy which is generated either by incandescence or luminescence. Incandescence is light from heat energy, i.e., heating an object at sufficiently high temperature that it begins to glow. Luminescence is known as “cold light”, which is light generated from alternative sources of energy, occurring at normal temperatures or even colder. The materials exhibiting luminescence are known as ‘Luminescent materials’ or ‘Phosphors’ meaning ‘light bearer’.

### 1.2.1. Classification of Luminescence

When excited electron reaches its ground state, it realizes its energy in the form of Radiative and Non-Radiative transitions. The non-radiative transition corresponds to the energy released in form of heat during electronic de-excitations. Radiative transitions correspond to luminescence process. Luminescence can be further classified depending upon its source of excitation as [2]: -

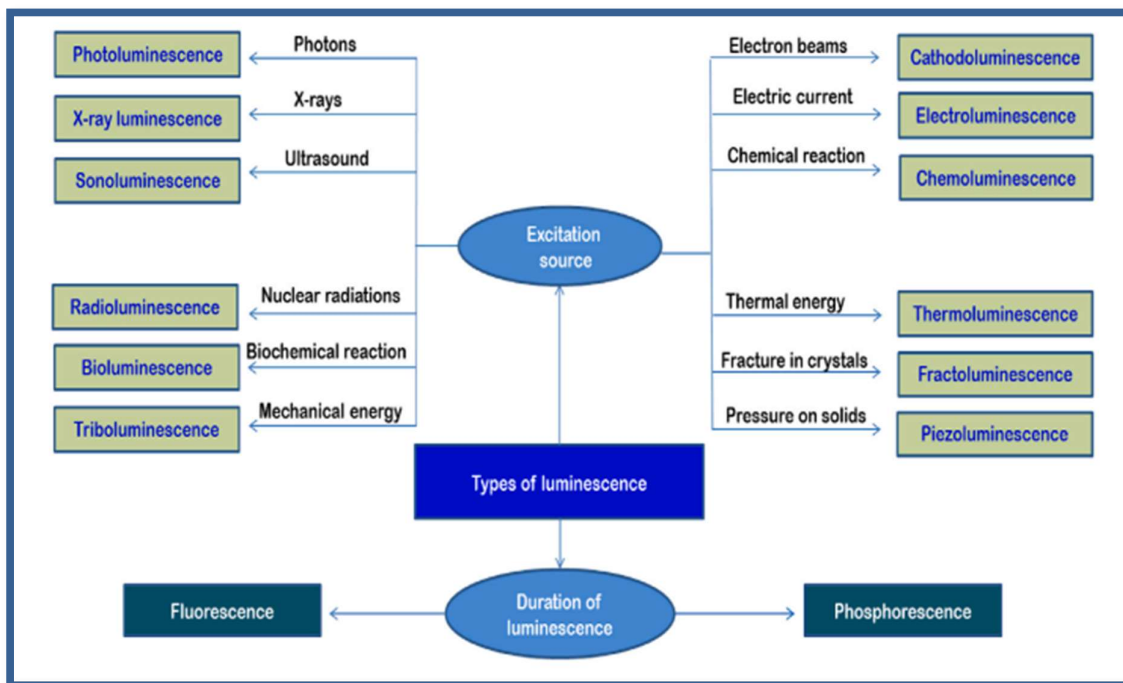


*Fig. 1.2. Types of luminescence based on different excitation sources and its duration*

- **Photoluminescence:** when light stimulates the luminescence process. It is of two types namely, fluorescence and phosphorescence.
- **Electroluminescence:** is a kind of luminescence in which the electric current works as source of excitation. TV, night lights, digital displays, etc are some of its applications.
- **Chemiluminescence:** is luminescence which is triggered as a result of chemical reactions. For example: Light from a glow stick, where a chemical reaction makes it glow.
- **Bioluminescence:** is actually a type of chemiluminescence. Light emission occurs from the body of living organisms like fireflies, some fungi, and many deep-sea creatures.
- **Thermoluminescence:** also known as thermally stimulated luminescence. It is used in archaeology for dating artifacts.
- **Radioluminescence:** when the sources of excitation are high energy X-rays or  $\gamma$ -rays. For example: Tritium excited luminous paints used on watch dials and gun sights.

### 1.2.2. Photoluminescence (PL)

Photoluminescence (PL) refers to emission of light by a material, induced by absorption of photon. It can be further classified into fluorescence and phosphorescence, on the basis of duration of emission [3].

#### 1.2.2.1. Fluorescence and Phosphorescence

After removal of excitation source, when immediate emission takes place (within  $10^{-8}$  seconds), it is referred as **fluorescence**. In case of **phosphorescence**, delayed emission takes place and it keeps on continuing after an extensive time interval of  $10^{-3}$  to 10 seconds to hours [4]. On a molecular level, *fluorescence* is light emission corresponding to transition between levels of same multiplicity. When it undergoes relaxation to the lowest vibrational level by *intersystem crossing*, light gets emitted due to electronic transition between levels of different multiplicity, causing **phosphorescence**. Fluorescence and phosphorescence correspond to

radiative processes while intersystem crossing, vibrational relaxation and internal conversion are non-radiative process [5].

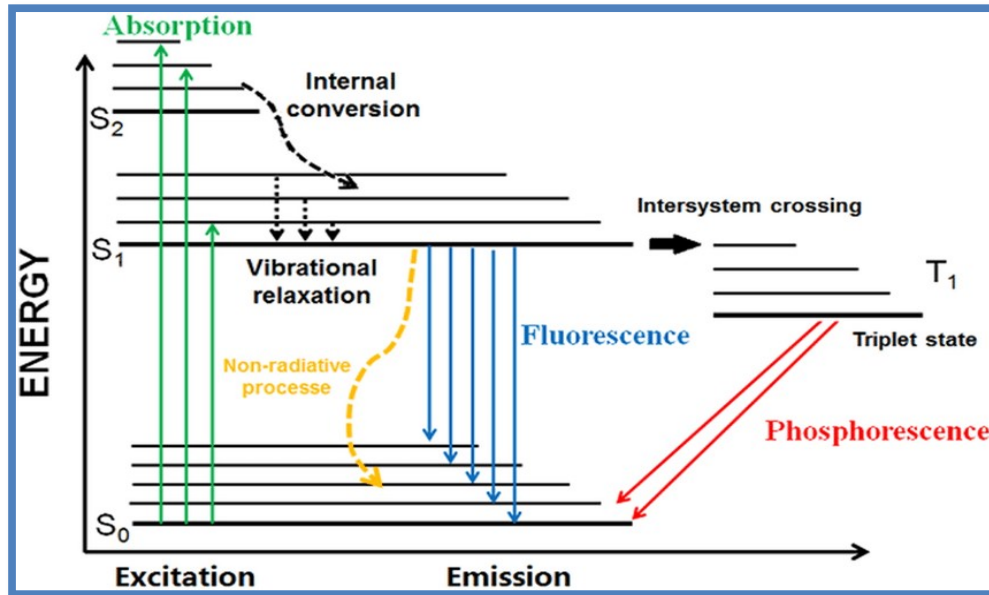


*Fig. 1.3. Jablonski Diagram for fluorescence and phosphorescence*

#### 1.2.2.2. Photoluminescence Process

The PL process takes place in the following sequence [4]:

- **Absorption:** A fraction of incoming photons from excitation source gets absorbed by electrons/ions present in the material. It is due to absorption, that incident radiations get attenuated after passing through material.
- **Excitation:** The absorbed energy by ions triggers them to undergo an electronic transition from their ground state to a higher excited state.
- **Relaxation:** Ions in their excited state return to ground state by release of energy to the lattice. The release of energy takes place either via phonons (non-radiative transition) or as emission of photons (radiative transition).
- **Non-radiative relaxation:** The lifetime of ions in the higher excited state is very short to obtain radiative emission. Due to proximity of higher energy levels to emitting states, the stimulated ions undergo relaxation to lower energy levels via release of heat or

lattice vibration (also known as phonons), leading to non-radiative relaxation or transition [3].

- **Radiative relaxation (Emission):** The de-excitation of ions from emitting state to ground state via release of photons is called as radiative relaxation or emission process. Such radiative process leads to photoluminescence [6, 7].

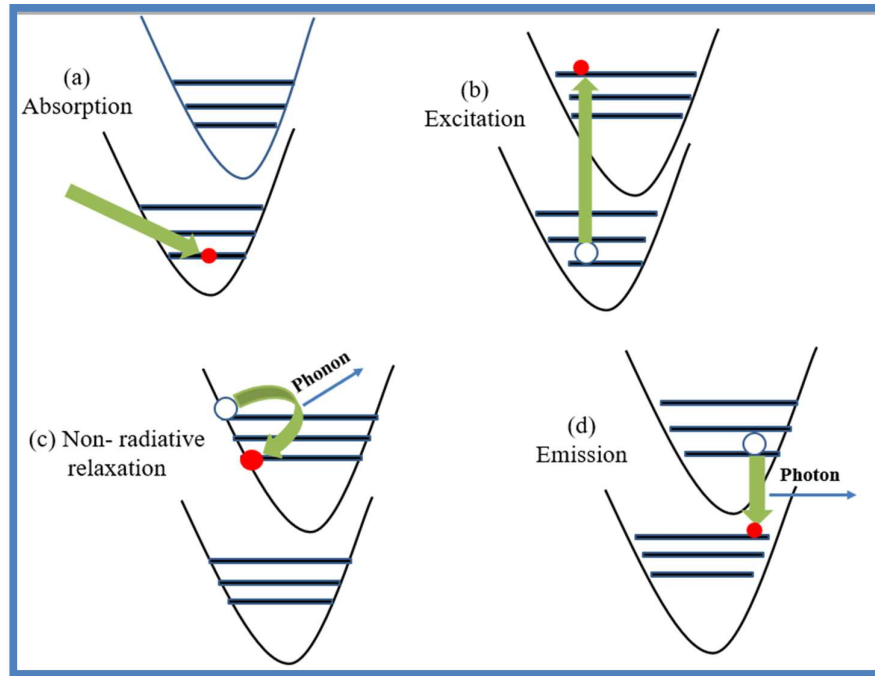


**Fig. 1.4. PL process (a) absorption, (b) excitation, (c) non-radiative relaxation, and (d) emission**

### 1.3. Rare Earth / Lanthanide Ions

Lanthanides are series of elements from lanthanum ( $^{57}\text{La}$ ) to lutetium ( $^{71}\text{Lu}$ ). Rare Earth (RE) is the name given to group consisting of all lanthanides, scandium ( $^{21}\text{Sc}$ ) and yttrium ( $^{39}\text{Y}$ ). The name “rare earth” is a bit deceptive as originally, the minerals (gadolinite and cerite) in which they were discovered are scarce, but not the elements. Thulium ( $^{69}\text{Tm}$ ) the least occurring lanthanide is more abundant than silver or cadmium. All members of RE family have their own specific physical properties, luminescent behaviour, colour, and nuclear magnetic properties [2]. The most stable oxidation state for RE ions is +3 with few exceptions that do

exist in +2 and +4 oxidation state due to their half-filled and fully-filled  $4f$  orbitals, such as in the case of  $\text{Eu}^{2+}$  and  $\text{Tb}^{4+}$  ions [8].

Name	Symbol	Atomic number	Electronic configuration	Oxidation state
Lanthanum	La	57	$[\text{Xe}] 5d^1 6s^2$	+3
Cerium	Ce	58	$[\text{Xe}] 4f^2 5d^0 6s^2$	+3, +4
Praseodymium	Pr	59	$[\text{Xe}] 4f^3 5d^0 6s^2$	+3, +4
Neodymium	Nd	60	$[\text{Xe}] 4f^4 5d^0 6s^2$	+2, +3, +4
Promethium	Pm	61	$[\text{Xe}] 4f^5 5d^0 6s^2$	+3
Samarium	Sm	62	$[\text{Xe}] 4f^6 5d^0 6s^2$	+2, +3
Europium	Eu	63	$[\text{Xe}] 4f^7 5d^0 6s^2$	+2, +3
Gadolinium	Gd	64	$[\text{Xe}] 4f^7 5d^1 6s^2$	+3
Terbium	Tb	65	$[\text{Xe}] 4f^9 5d^0 6s^2$	+3, +4
Dysprosium	Dy	66	$[\text{Xe}] 4f^{10} 5d^0 6s^2$	+3, +4
Holmium	Ho	67	$[\text{Xe}] 4f^{11} 5d^0 6s^2$	+3
Erbium	Er	68	$[\text{Xe}] 4f^{12} 5d^0 6s^2$	+3
Thulium	Tm	69	$[\text{Xe}] 4f^{13} 5d^0 6s^2$	+2, +3
Ytterbium	Yb	70	$[\text{Xe}] 4f^{14} 5d^0 6s^2$	+2, +3
Lutetium	Lu	71	$[\text{Xe}] 4f^{14} 5d^1 6s^2$	+3

**Fig. 1.5. Rare earth ions with their electronic configuration and oxidation state**

Luminescence in lanthanides arise due to electronic transitions within their  $4f$  orbitals. These distinct optical properties are a result of screening of partially filled  $4f$  orbital by completely filled  $5s$  and  $5p$  orbitals [9]. Each of them has their own characteristic energy level and emission profile. For example: europium ( $\text{Eu}^{3+}$ ) radiates red light, terbium ( $\text{Tb}^{3+}$ ) release green light, gadolinium ( $\text{Gd}^{3+}$ ) emits in the ultraviolet region, and erbium ( $\text{Er}^{3+}$ ) in the near-infrared region [8]. Lately, RE ions have gained much attention due to their unique physical, chemical, magnetic, and luminescent properties. They provide reduced energy consumption, greater efficiency, durability, and thermal stability. Application of RE element includes optical



glass, fiber optics, various display devices, medical diagnosis, rechargeable batteries, light emitting diodes (LEDs), computer memory, lasers, etc [2].

### ***1.3.1. Unique Features of Rare Earth Ions***

Rare Earth (RE) ions reveal distinctive features that differentiate between RE ions and other optically active ions. Some of these properties are [6]:

- RE ions show narrow spectral lines that implies monochromatic light with longer emission lifetime.
- They display luminescence in the electromagnetic spectrum's visible and near infrared spectral ranges.
- RE ions possess several excited levels suitable for optical pumping.
- They exhibit large stokes shift upon excitation (due to huge gap between excitation and emission spectra).
- Their intra-configurational 4f transitions have small homogenous linewidths.

### **1.4. Phosphor and Luminescence Mechanism**

Phosphors are light emissive material. They convert the absorbed energy into light, without undergoing incandescence. Phosphor materials are generally inorganic material with an average particle size ranging from  $10^{-6}$  ( $\mu\text{m}$ ) to  $10^{-9}$  (nm). The most commonly used phosphor are composites of silicates, halides, borates, oxide, sulfide, and oxynitride. It consists of a host matrix, where dopant or activator ion is substituted. The activator ion could be a rare earth ion or transition metal. An ideal host matrix has a low cut-off phonon frequency, high thermal stability, broad transparency range, and a tunable crystal phase.

The process of luminescence in phosphor involves absorption of energy from source of excitation, followed by relaxation to ground state and subsequent emission of photons in the visible region. Energy is either absorbed by activator ion or the host lattice which later transfer the energy to activator present in the matrix. Due to absorption, electrons of the activator ion get excited and then return to their ground state via either emission of light or emission of phonon. For the latter, energy is released as a form of heat and former results in luminescence. The light emission occurs from a luminescent center and in case of phosphors, the activator ion incorporated in the host lattice acts as the luminescent center. Sometimes activator ion exhibits weak absorption, in such case co-dopants (called as sensitizers) are also doped into the matrix along with activator ions. The energy gets absorbed by sensitizer and is then transferred to activator for luminescence [9, 10].

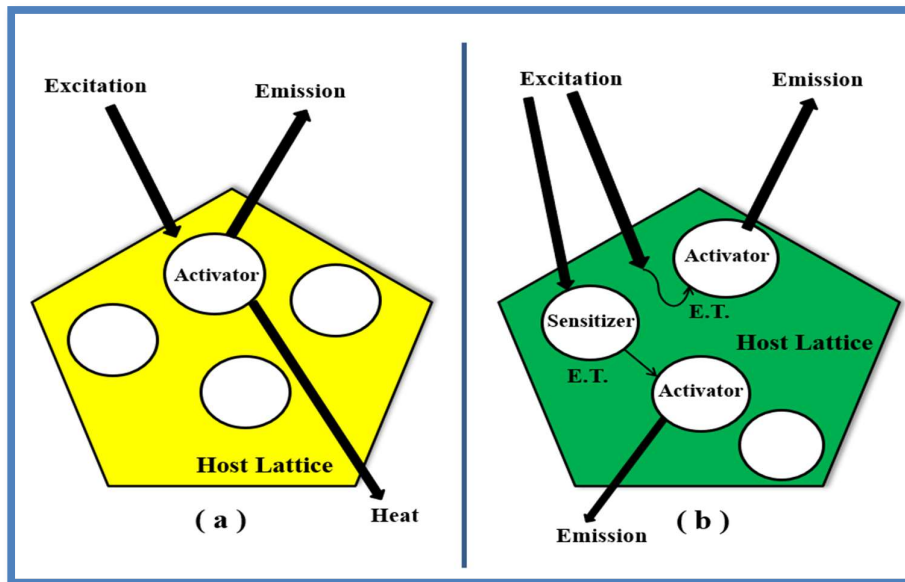


**Fig. 1.6. (a) Direct absorption via activator, and (b) energy transfer (ET) by host or sensitizer to activator**

### 1.5. Application: White Light Emitting Diodes (w-LEDs)

Energy is an essential commodity in the modern world. Hence, there exist the scientific quest for achieving the most energy efficient lightning device. Lightning applications involving light emitting diodes (LEDs), organic LEDs or light emitting polymers are commonly referred

to as Solid State Lighting (SSL) devices. The high efficiency, longer lifetime, compact structure, and cost saving attributes of SSL devices have enabled them to replace conventional light sources like incandescent bulb and fluorescent lamp [11, 12]. In this context, white light emitting diodes (w-LEDs) emerges as a crucial component of SSL technology. There are different approaches for generation of white light using LEDs.

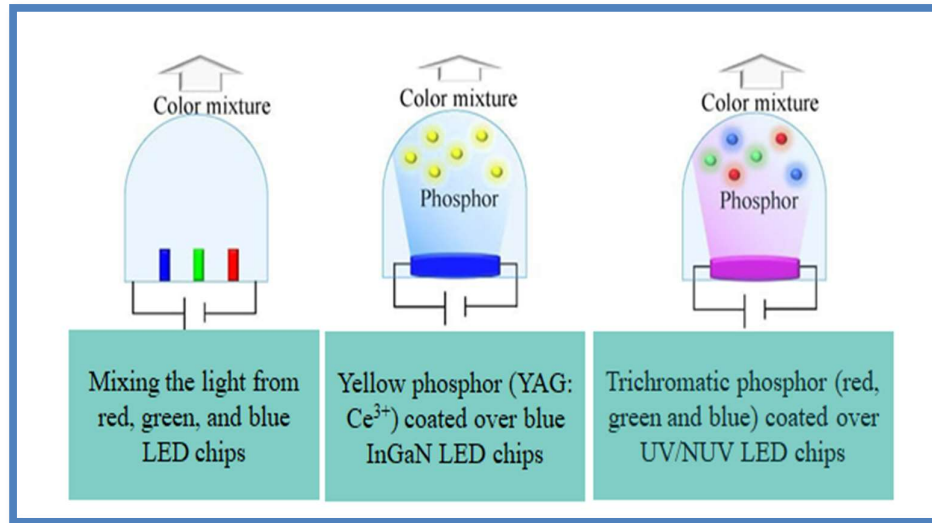


**Fig. 1.7. Different approaches for white light generation via LEDs**

The first approach is to use combination monochromatic red, green and blue LEDs, so as to produce white light. Both this approach requires different driving current for individual LEDs and also exhibit instability of color temperature. The other two approaches are known as phosphor converted white light emitting diodes (pc w-LEDs) [13]. Commercially available pc w-LEDs is fabricated by coating a yellow phosphor ( $\text{Y}_3\text{Al}_5\text{O}_{12}:\text{Ce}^{3+}$ ), over blue light emitting (InGaN) LED chip. But due to shortage of red component in the emissive light, it results in low color rendering index (CRI) value, high correlated color temperature (CCT), and weak thermal stability [14]. Another approach is to coat tricolour phosphor (red, green and blue) over near ultraviolet LED chips. This approach yields high efficiency, enhanced chromatic stability and CRI values along with dealing with the shortage of red component in the white light generated [3].

### 1.5.1. Colorimetry Properties

Important factors including luminescence efficiency, correlated color temperature (CCT) values, and Common Internationale de l'Eclairage (CIE) coordinates influences a phosphor material's luminescence performance.

International Commission on Illumination generated color model such as CIE 1931, CIE 1960 and CIE 1976 to represent the color space [15]. The human eye produces each color using red, green and blue (RGB) cone cells, similarly the color model makes use of 3-D representation of RGB (tristimulus values) to evaluate the appropriate color array for various display applications. The color parameters are calculated using the data from the emission profile of the material. The tristimulus function  $\bar{x}(\lambda)$ ,  $\bar{y}(\lambda)$  and  $\bar{z}(\lambda)$  evaluates the parameters X, Y and Z. The CIE coordinates (x and y) represents the position for corresponding color in the chromaticity chart. Tristimulus values are converted to chromaticity coordinates via following equation:

$$x = \frac{X}{X+Y+Z} \text{ and } y = \frac{Y}{X+Y+Z} \quad (1)$$

Correlated color temperature (CCT) defines the warmth or coolness of light. It describes the color temperature of light source by correlating it with the temperature of ideal blackbody radiator and is measured in the units of kelvin (K).



**Fig. 1.8. CCT scale**

Lower CCT values refer warmer light used in restaurants and hotels. While higher value denotes cooler light used in workplaces. Light source with a CCT value  $< 5000$ , K are suitable for warm light application while those with CCT values  $> 5000$  K, are more effective for cool light applications. The ability of light source to render all colours of an object that is being illuminated is given by color rendering index (CRI) and is denoted by  $R_a$ . Natural sunlight has a CRI score of 100 as it perfectly portrays the object. Thus, possessing a higher value of CRI score is an essential criterion for any light source. Luminous efficacy measures how effectively do a light source converts electrical energy into light. It is denoted by (K) and is defined as the ratio of total light output in lumens to the power (watts or equivalent) [9, 16].

### **1.6. Motivation & Objectives**

In today's world, where the focus is on environmental considerations and sustainability. The research interest has been pivoted towards development of white light emitting diodes (w-LEDs) for solid state lighting applications. The commercially available phosphor converted w-LEDs (pc w-LEDs) are fabricated by coating yellow phosphor  $Y_3Al_5O_{12}: Ce^{3+}$  (YAG:  $Ce^{3+}$ ) over InGaN blue LED chip. However, the light generated from these commercially available pc w-LEDs possess a poor color rendering index (CRI) value and a high correlated color temperature (CCT) due to shortage of red color in their emission profile [17]. Therefore, to overcome these limitations, it is essential to develop a novel red emitting phosphor with exceptional thermal and chemical stability.

Rare earth (RE) doped phosphor has recently been the subject of extensive research due to its remarkable chemical stability and environmentally friendly optical characteristics. The development of inorganic oxide-based host lattice has resulted in advancement of modern-day display applications. Yttrium niobium titanate,  $YNbTiO_6$  (YNT) has gained much attention as a host matrix due to its excellent thermal and chemical stability, luminescence properties and environmentally friendly characteristics [18].

RE ions are most commonly used activators ions due to their distinctive luminescence features owing to the intra configurational 4f transitions. Subsequently, by adding the proper dopants to the host matrix, emissive color phosphor material can be modified.  $\text{Eu}^{3+}$  doped phosphor exhibits a perfect red color component with high purity, arising due to  ${}^5\text{D}_0 \rightarrow {}^7\text{F}_2$  transition and emission wavelength of  $\sim 612$  nm [9].

The main objectives of present work are:

1. To synthesize a novel red emitting phosphor material via solid state reaction method.
2. To study the structural and morphological properties of as-synthesised phosphor.
3. To investigate the luminescent characteristics of europium ( $\text{Eu}^{3+}$ ) induced YNT phosphor
4. To determine the colorimetric properties of the  $\text{Eu}^{3+}$  induced YNT phosphor.
5. To explore the potential use of  $\text{Eu}^{3+}$  doped YNT phosphor as a red-emitting component for w-LED applications.

## CHAPTER 2: SYNTHESIS AND EXPERIMENTAL PROCEDURE

### 2.1. Synthesis Methods

The synthesis route is a necessary requirement that determines the size, shape, distribution and structure of the material. Phosphor materials can be produced by using various physical and chemical methods of preparation. According to literature, the following are some various physical synthesis techniques [7].

#### 2.1.1. Solid State Reaction (SSR) Method

It is a common synthesis method with high-temperature for producing materials, where the reactants are solid at room temperature. This method involves the direct reaction between solid reactants at elevated temperatures, leading to the formation of a product without the need for a solvent. It is a simple process with easy scalability in terms of production of sample [19]. Synthesis procedure begins with considering high purity oxide materials as precursors. Precursors are then weighed according to the stoichiometric calculations and grounded into a fine powder using agate motor and pestle. During mixing, acetone is used as dispersing medium for obtaining a homogenous mixture. The grounded sample is placed in crucibles (made of platinum/alumina) and heated at high temperature for a period of time [20-22].

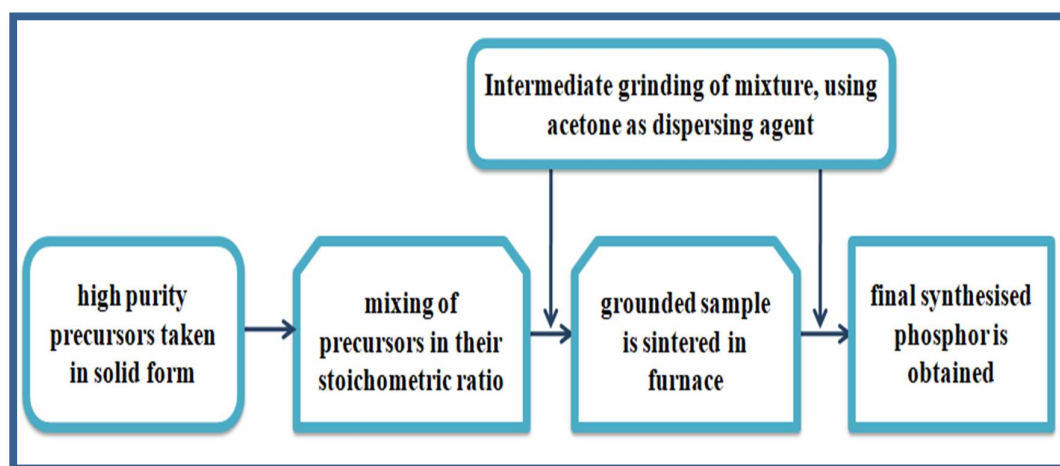


*Fig. 2.1. Steps involved in solid state reaction method*

Surface area of solid reactant (precursor), reaction conditions, structure reactivity of precursor along with thermodynamic free energy change are some of the important parameters affecting the feasibility and rate of synthesis process. Extra milling is required to produce desirable final product [23].

### 2.1.2. Sol-Gel Method

The sol-gel method is a popular and effective process for the synthesis of glasses and ceramic materials such as metal oxides, nitrides and carbides. This method involves conversion of a sol (colloidal solution) into a gel-like network, followed by further processing to create the desired material.

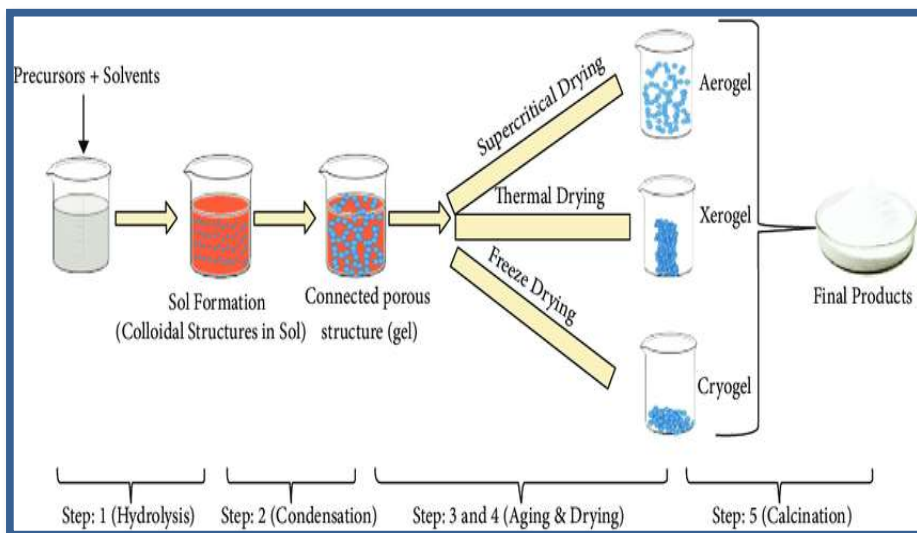


**Fig. 2.2. Steps involved in sol-gel process of material synthesis**

Compared to conventional processing methods, this methodology offers a number of advantages including the capacity to build processes for large-area applications, strong composition control, high purity levels and the ability to incorporate components that are sensitive to temperature due to its low reaction temperature [24]. Sol or colloidal solution is formed by dissolution of solvent. Characteristic properties of the final product, decides the solvent chosen. Gel is formed as a result of hydrolysis and condensation of sol. Wet gel can be dried up by employing different drying methods. In case of thermal drying xerogel is formed,



from supercritical drying aerogel is formed and from freeze drying cryogel is formed. The choice of drying method influences the properties of the final material. The dried gel undergoes heat treatment, such as calcination or sintering. Heat treatment is required for the removal of any remaining component and promotes crystallization of products. By changing the chemical conditions of polymerization, the structure and the morphology of samples formed are drastically affected [25-27].

### **2.1.3. Hydrothermal Method**

The hydrothermal process allows for the formation of crystalline materials with controlled structures, sizes and properties. The term ‘hydrothermal’ originates from earth science. Our planet itself is a huge hydrothermal vessel, in which some precious crystals such as quartz crystal are formed. Here, the growth of crystal takes place in a device consisting of steel pressure vessel called an autoclave (reaction vessel capable of withstanding high pressure), in which a nutrient is supplied along with water. The opposite ends of growth chamber have a temperature gradient. For the formation of desired crystal, nutrient solute dissolves at hotter end while gets deposited at the cooler end. After a specific duration, the autoclave cools down to room temperature. This controlled cooling is essential for the formation of well-defined crystals and the prevention of rapid quenching effects. The synthesized material is then collected, typically through filtration or other separation techniques. The collected material may be in the form of powders, particles or larger structures, depending on the specific synthesis condition. Type of solvent, temperature, reaction condition and its duration play a significant role in the overall synthesis process. Nucleation and gain growth controls the particle size of the final product. Effective dispersion in solution, streamlined one-step synthesis process, economically feasible in terms of instrumentation used, environmental friendliness and gentle operating conditions are some of the few advantages of hydrothermal synthesis route [28-30].

### 2.1.4. Molten Salt Synthesis

Molten Salt Synthesis (MSS) is one of the most effective bottom-up synthesis techniques. During synthesis, ionic molten salts are used at low temperature. Here, most of the metal ions or bonds might get destabilized by solvents of high polarisation at high temperature. The efficient removal of residual product at the end of reaction is achieved as a result of high aqueous solubility of molten salts.

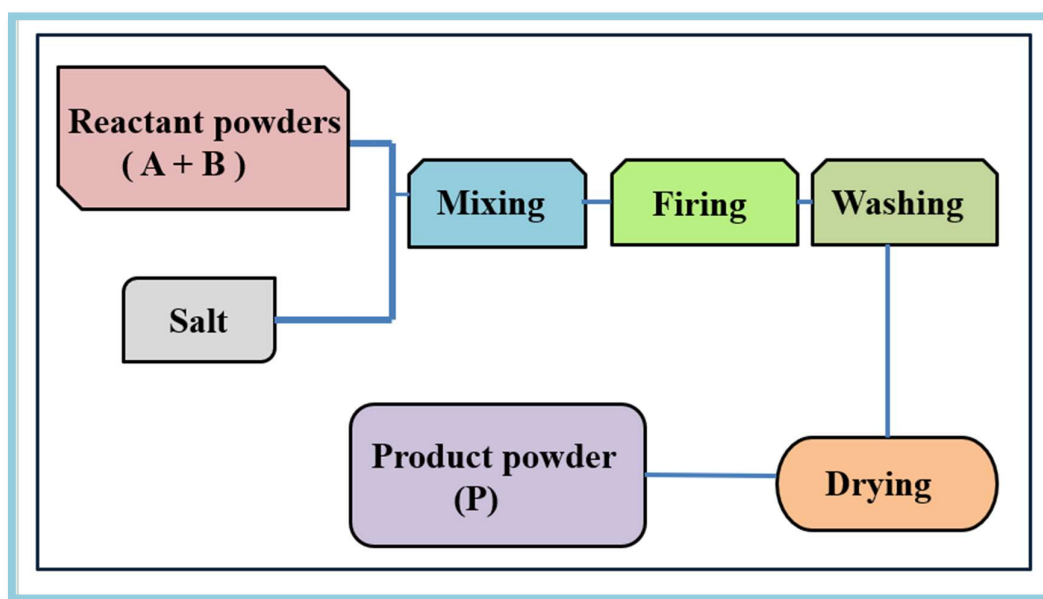


*Fig. 2.3. Steps involved in molten salt synthesis*

MSS is a desirable synthesis technique owing to its easy scalability and clean methodology of preparation, also making it economical for industrial purpose. However, the molten solid-state method may require careful control of temperature and reaction conditions to achieve the desired results [31, 32].

### 2.1.5. Co-precipitation Method

To prepare multi component materials via formation of intermediate precipitates whose chemical homogeneity is then maintained during calcination, we use Co-precipitation method. It is often employed for the synthesis of metal oxides, hydroxides, and other compounds. In the

typical process of co-precipitation, two or more precursor salts are dissolved in a suitable solvent to form a homogeneous solution. A precipitating agent is added to the precursor solution to induce the formation of solid particles. This reaction leads to the formation of solid particles in the solution. These particles are often formed in the form of colloidal suspensions. In some cases, the dried powder may undergo calcination or heat treatment at elevated temperatures. This step is carried out to remove residual organics, enhance crystallinity, and induce phase transformations in the material. The crystalline size obtained using co-precipitation method is smaller as compared to other synthesis routes. Continuous washing, drying and calcination of material contribute to be one of the major drawbacks of this method [33-35].

## 2.2. Synthesis of Phosphor Material

### 2.2.1. Selection of Host Matrix

The selection of suitable host matrix plays an important role in development of a stable and efficient phosphor material. Typical titaniniobates with the general formula  $RENbTiO_6$ ,  $RE = Y$  ( $YNbTiO_6$ ), which belongs to the orthorhombic euxenite-type family with space group  $Pbcn$  have sparked a lot of attention because of their potential use as a host lattice for luminescent material [36].

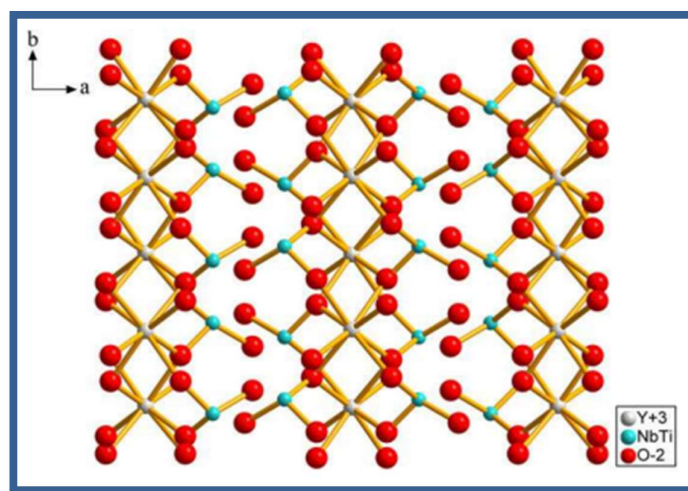


Fig. 2.4. Crystal structure of euxenite type  $YNbTiO_6$

The YNbTiO<sub>6</sub> (YNT) lattice comprises of deformed Nb(Ti)O<sub>6</sub> octahedra double layers joined together via edge and corner sharing, along with an irregular single layer of YO<sub>8</sub><sup>13-</sup> polyhedron dividing the neighbouring Nb(Ti)O<sub>6</sub> as shown in **Fig. 2.4**. YNT can be regarded as a valuable luminous host lattice because of its excellent chemical and thermal stability as well as optical properties [37, 18]. Moreover, it also serves as the suitable host lattice for doping of trivalent rare earth ions (RE<sup>3+</sup>) since it allows for their substitution of Y<sup>3+</sup> sites without any requirement for charge compensation [38].

### ***2.2.2. Selection of Synthesis Route: SSR Method***

The solid-state reaction (SSR) method is a simple synthesis route which is widely used due to its simplicity, affordable starting materials, large-scale production, high surface area of products, “clean” reactions devoid of additional elements, and the ease with which host lattice defects can be introduced. It is favoured most for its efficiency, and ability to produce materials with desired physical and chemical properties. This template-free nature allows the material to develop its intrinsic morphology based on the interactions between the reactants, providing greater flexibility in tailoring the final product’s shape and structure. It involves direct reaction of solid reactants at high temperature without the need for any solvent. The elevated temperature promotes diffusion of reactant species, allowing atoms or ions to move and rearrange themselves in a controlled manner.

### ***2.2.3. Sample Preparation***

YNbTiO<sub>6</sub> (YNT) host lattice and YNT: xEu<sup>3+</sup>, x = 1.0 mol% phosphor has been synthesised by using precursors of high purity (≥ 99.99%). The starting ingredients, yttrium oxide (Y<sub>2</sub>O<sub>3</sub>), niobium pentoxide (Nb<sub>2</sub>O<sub>5</sub>), titanium dioxide (TiO<sub>2</sub>) and europium (III) oxide (Eu<sub>2</sub>O<sub>3</sub>) were taken in stoichiometric proportion. Precursors were grounded using agate motor and pestle, with acetone as a dispersing agent to achieve a uniform mixture. Further, the mixture was transferred into alumina crucible and calcinated at 1300 °C for 4 hours in a temperature

controlled programmable furnace. The sample was allowed to cooled down to room temperature. Thereafter, it was further milled into fine size for further characterization purpose.

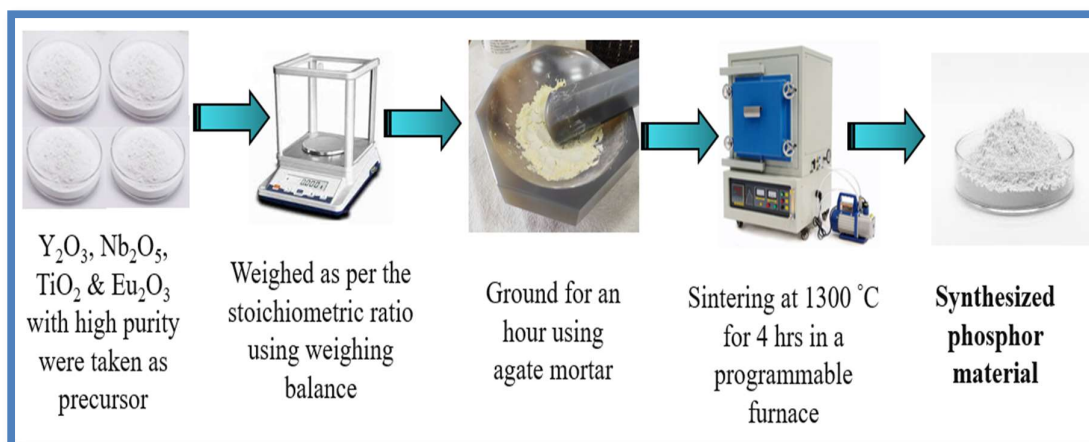


**Fig. 2.5. Steps for synthesis of YNT:  $x\text{Eu}^{3+}$  ( $x = 1.0$  mol%) phosphor via SSR method**

#### **2.2.4. Analysis of Sample**

A high-resolution diffractometer (Rigaku Smart lab) with  $\text{CuK}\alpha$  ( $\lambda = 1.5406 \text{ \AA}$ ) radiation source was employed to study the structure and phase purity of the synthesized YNT:  $x\text{Eu}^{3+}$  ( $x = 1.0$  mol%) phosphor in the  $2\theta$  range from 20 to 60 °. The morphological analysis of host lattice has been evaluated via the use of field emission scanning electron microscope (FE-SEM) Model: Zeiss GeminiSEM 500. Furthermore, the photoluminescent properties (PLE and PL) of the prepared phosphor material has been captured using a JASCO-8300FL spectrophotometer. All the above-mentioned characterization tools have been accomplished under room temperature.

## CHAPTER 3: CHARACTERIZATION TECHNIQUES

### 3.1. Characterization Techniques

#### 3.1.1. X-Ray Diffraction

X-ray crystallography is a method of determining the arrangement of atoms within a crystal. X-ray diffraction analysis (XRD) involves exposing the substance to incoming X-rays and examining the intensity and scattering trajectory of the radiation. Fig. 3.1 depicts the X-ray diffraction machine used for characterization.



*Fig. 3.1. X-ray diffraction Machine*

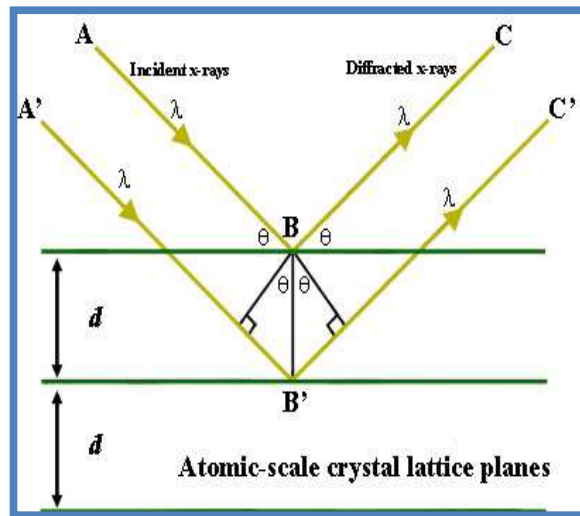


*Fig. 3.2. Bragg's Law*

The length between lattice planes in crystalline materials and the X-ray wavelengths are of comparable magnitude. The atoms' surrounding electron clusters will distribute the X-rays when they enter the substance. As depicted in Fig. 3.2, the X-rays' constructive interference is caused by the periodicity of planes within the lattice, and a plot of the intensity of the scattered X-rays versus  $2\theta$  confirms this Bragg's law. Bragg's law as shown by equation (3.1)

$$2d \sin \theta = n\lambda \quad (3.1)$$

Here  $d$  is the spacing between crystal lattice planes or diffracting planes,  $\theta$  is the incident angle,  $n$  is any integer, and  $\lambda$  is the wavelength of the beam [10, 39].

#### **3.1.1.1. *Joint Committee on Powder Diffraction Standards (JCPDS)***

An extensive database of diffraction patterns and related data for a variety of crystalline materials is made available by the Joint Committee on Powder Diffraction Standards (JCPDS), which was founded in 1941. The powder diffraction file contains diffraction data, sample needs, research and literature data, crystallographic, and desirable mechanical properties in a conventional graded format. In order to create the International Centre for Diffraction Data (ICDD), the American Society for Testing and Materials (ASTM) and the International Centre for Diffraction Data (ICDD) joined with the JCPDS in 1989 [10, 39].

#### **3.1.2. *Field Emission Scanning Electron Microscopy (FE-SEM)***

Field emission scanning electron microscopy (FE-SEM) is an advanced imaging technique utilized to produce high resolution images of material surfaces. It provides detailed morphology of the material. As the name suggest, it employs a field emission gun as a source of electron, unlike conventional scanning electron microscopy (SEM) that uses thermal electron sources. Resolution of image is in case of FE-SEM than SEM because both backscattered and secondary electrons, are employed in FE-SEM [40]. The emitted secondary electrons are collected by a detector, and their intensity variations are translated into an image. This method offers superior depth of field, allowing clearer imaging of three-dimensional. FE-SEM is also used to yield better, low voltage imaging with minimal electrical sample charging and damage, thus preventing the integrity of sample. Yet another benefit of FE-SEM is the fact that, insulating materials do not always require a coating of conductive material [41]. The set up for FES-SEM is shown by Fig. 3.3.

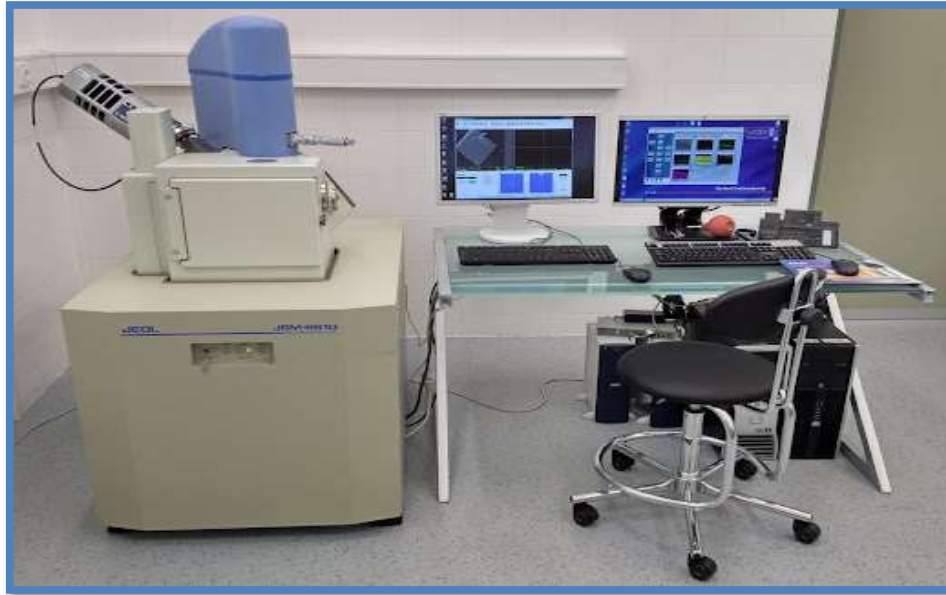


***Fig. 3.3. FE-SEM (Zeiss GeminiSEM 500)***

### ***3.1.3. Photoluminescence (PL) Spectroscopy***

Photoluminescence spectroscopy provides a non-contact and non-destructive exploration of the luminescent properties. It is based on the principle of photoluminescence. The plot between intensity of emitted light and wavelength provides the photoluminescence spectrum [7]. The intensified emission peaks in the PL spectrum reflects towards the energy level necessary for excitation, which further provides insights into the exact emission spectrum of the phosphor material. Both excitation and emission spectra, the intensity is plotted along the ordinate (y-axis) and wavelength along abscissa (x-axis) [6].



***Fig. 3.4. PL (JASCO-8300FL) Spectrophotometer***



Fig. 3.4. exhibits the spectrophotometer used for present thesis work. The PL spectrophotometer comprises of an excitation light source, monochromator, photodetector, amplifier, etc connected to computer. The PL spectroscopy analysis involves various step:

**1. Excitation:** The source of excitation should yield a continuum spectrum instead of line spectra. Xenon lamp provides a moderately continuous light output. A monochromator is associated with the assembly which allows only selected wavelength of light. The light from excitation monochromator is flashed over the phosphor sample.

**2. Absorption, Relaxation and Emission:** On absorption of photons, electrons get excited to higher energy states. Upon radiative relaxation of excited carriers, photons are emitted. Emitted light is preferably in the visible region. Detection and Analysis: The emitted light is detected by photomultiplier tube (PMT). MT amplifies the detected signal and then convert it into a signal form and computer screen displays the recorded spectrum in terms of intensity as a function of wavelength.

PL spectroscopy offers applicability in fields of environmental sciences, medical diagnostics, cell biology, and molecular electronics. During PL measurement we can also change other external parameters such as temperature, pressure, external perturbation so that we can get more investigation about electronic states, band structure, and carrier dynamics [4].

## CHAPTER 4: RESULTS AND DISCUSSION

### 4.1. Europium ( $\text{Eu}^{3+}$ ) doped Yttrium Niobium Titanate (YNT) Phosphor

#### 4.1.1. Structural Studies

X-ray diffraction (XRD) profiles have been applied to analyze the structural and phase purity of the synthesized YNT host lattice and YNT:  $x\text{Eu}^{3+}$ ,  $x = 1.0$  mol% sample. The diffraction profiles of synthesized host lattice, YNT:  $x\text{Eu}^{3+}$  sample and along with standard JCPDS data, as illustrated in Fig. 4.1. It has been observed that the patterns of JCPDS card no. 01-083-1318 were found to be well-matched with all of the indexed diffraction peaks. The analysis of the synthesized host lattice to standard data indicated that the  $\text{YNbTiO}_6$  crystal structure is orthorhombic, with the  $Pbcn$  space group [42]. The highest diffraction peak was indexed as (311) crystallographic plane, which was observed at a  $2\theta$  value of  $29.85^\circ$ . Furthermore, the diffraction profile of the synthesized YNT:  $x\text{Eu}^{3+}$ , where  $x = 1.0$  mol% sample is exactly consistent with standard JCPDS data, with no impurity peaks. This confirms that the  $\text{Eu}^{3+}$  ions were efficiently incorporated in the YNT host lattice.

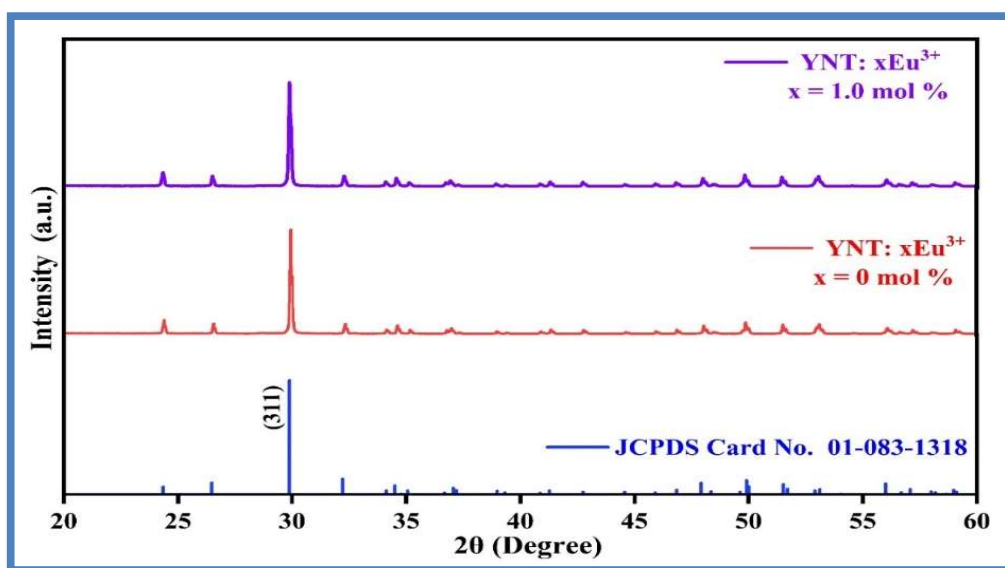


Fig. 4.1. Diffraction patterns of YNT host lattice & YNT: 1.0 mol%  $\text{Eu}^{3+}$  phosphor

In the  $\text{YNbTiO}_6$  host lattice, the  $\text{Eu}^{3+}$  ions occupied the  $\text{Y}^{3+}$  site since the effective ionic radii of  $\text{Eu}^{3+}$  ions ( $r = 0.94 \text{ \AA}$ ) are slightly less than that of the  $\text{Y}^{3+}$  ( $r = 1.02 \text{ \AA}$ ) ions. The average crystallite size ( $D$ ) for the YNT host lattice and YNT:  $x\text{Eu}^{3+}$  sample has been computed via applying the Debye–Scherrer equation as given below [43, 44]:

$$D = \frac{K\lambda}{\beta \cos\theta} \quad (4.1)$$

The full width at half maximum (FWHM) of the strong diffraction peak is represented as  $\beta$ . The X-ray used with a wavelength of  $1.5406 \text{ \AA}$ , is denoted as  $\lambda$ . The diffraction angle is signified as  $\theta$ .  $K$  is the shape factor and its value is 0.94. The crystallite size ( $D$ ) for the synthesized YNT host lattice and YNT:  $x\text{Eu}^{3+}$ ,  $x = 1.0 \text{ mol\%}$  sample has been computed in the range of 50-65 nm.

#### 4.1.2. Morphological Studies

Fig. 4.2. depicts the surface morphology of the synthesized  $\text{YNbTiO}_6$  (YNT) host lattice. FE-SEM micrograph indicates the irregular/asymmetrical morphology of the YNT host lattice with particle size in the micron range.

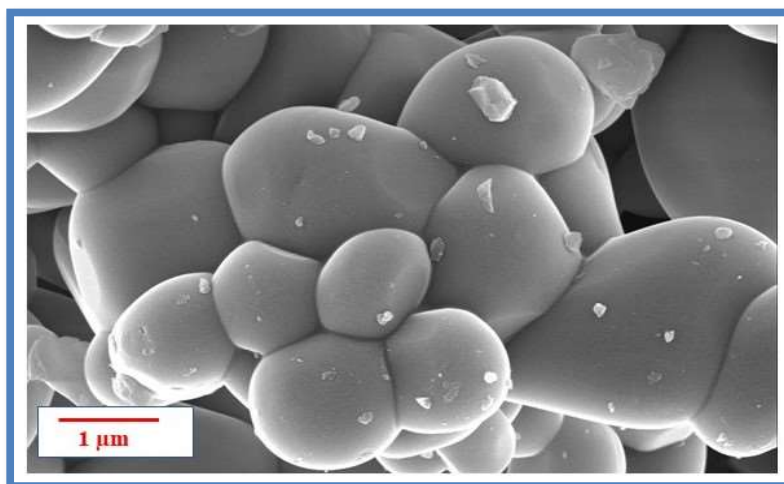


*Fig. 4.2. FE-SEM micrograph for YNT host.*

### 4.1.3. Photoluminescence Studies

In order to understand the detailed emission spectral characteristics of the YNT: Eu<sup>3+</sup> phosphor, it is necessary to be stimulated with an appropriate excitation wavelength, and an excitation spectrum has to be captured by keeping the dominant emission wavelength of the dopant (Eu<sup>3+</sup>) ions. The photoluminescence excitation (PLE) spectrum of the synthesized YNT: xEu<sup>3+</sup> phosphor has been performed in the spectral range of 240 to 500 nm via fixing an intense emission wavelength of 612 nm. The PLE spectrum for synthesized YNT: xEu<sup>3+</sup>, x = 1.0 mol% is illustrated in Fig. 4.3. A broad intense peak has been observed around 280 nm associated with the charge transfer band (CTB). As shown in inset Fig. 4.3., several other excitation peaks around 363, 382, 394, 417, and 465 nm are related to the transitions of Eu<sup>3+</sup> at  ${}^7F_0 \rightarrow {}^5D_4$ ,  ${}^7F_0 \rightarrow {}^5L_7$ ,  ${}^7F_0 \rightarrow {}^5L_6$ ,  ${}^7F_0 \rightarrow {}^5D_3$  and  ${}^7F_0 \rightarrow {}^5D_2$ , respectively [45-48].

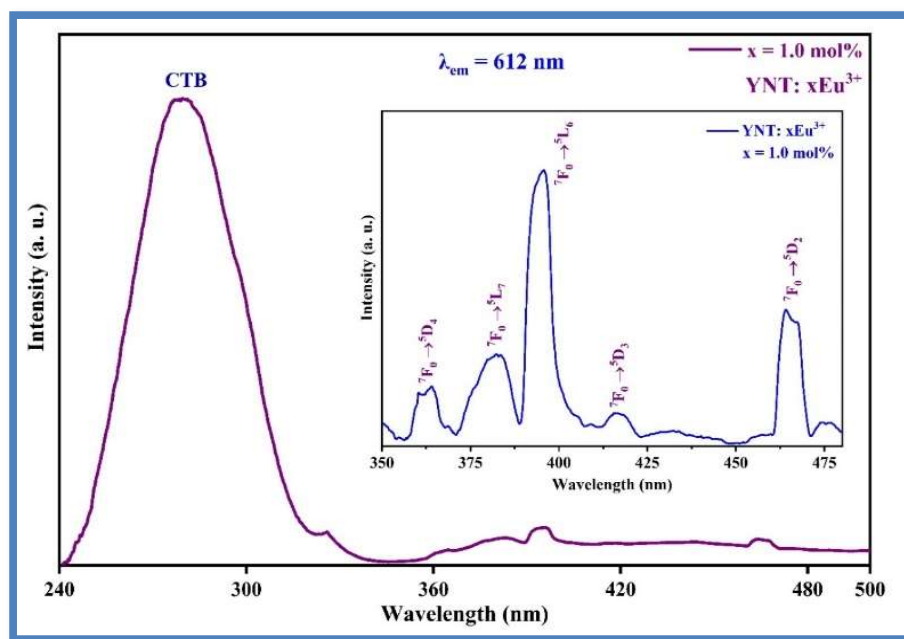


**Fig. 4.3. PLE spectrum of the YNT: 1.0 mol% Eu<sup>3+</sup> phosphor under  $\lambda_{em}=612$  nm (Inset represents the PLE spectrum in the 340 to 480 nm range.)**

Among all the PLE peaks, three intense excitation peaks have been observed in the regions of ultraviolet (UV) at 280 nm, n-UV at 394 nm and blue at 465 nm associated with the CTB,

${}^7F_0 \rightarrow {}^5L_6$  and  ${}^7F_0 \rightarrow {}^5D_2$  transitions, respectively. Thus, the PLE spectrum confirms that the YNT:  $x\text{Eu}^{3+}$  phosphor can be proficiently stimulated via UV, n-UV and blue light.

The emission profile of the synthesized YNT:  $x\text{Eu}^{3+}$ ,  $x = 1.0$  mol% phosphor has been captured at room temperature via fixing the excitation wavelengths of UV, n-UV and blue light. Fig. 4.4. illustrates the emission spectrum of YNT: 1.0 mol%  $\text{Eu}^{3+}$  phosphor and was captured in the wavelength range of 400 to 750 nm under the excitation wavelength of UV light. It has been observed that a broad emission peak has been detected in the 420 to 575 nm range due to the recombination of intrinsic self-trapped excitons (STEs) in the YNT host lattice [18]. Also, several other emission peaks have been observed due to dopant ( $\text{Eu}^{3+}$ ) ions in the range from 550 to 750 nm. The detected emission peaks are located at 592, 612, 655 and 703 nm, which are related to the  ${}^5D_0 \rightarrow {}^7F_J$  (where  $J = 1$  to 4) transitions, respectively [47, 48].

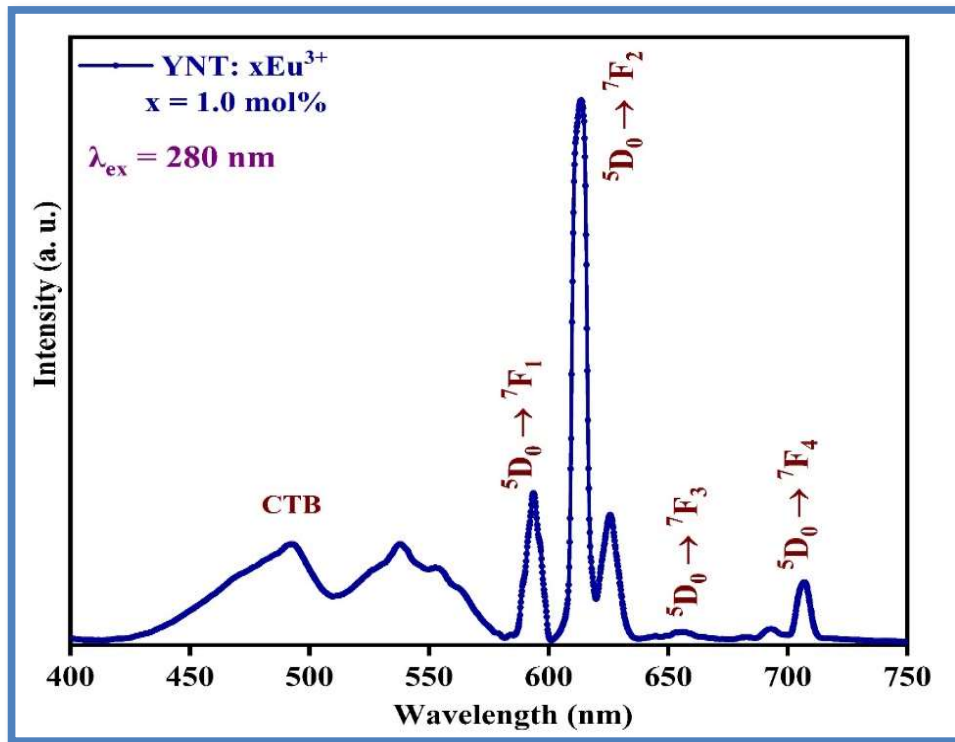


*Fig. 4.4. PL spectrum of the YNT: 1.0 mol%  $\text{Eu}^{3+}$  phosphor under  $\lambda_{exc} = 280$  nm*

Furthermore, the emission spectra of the synthesized phosphor were measured by keeping the excitation wavelengths of n-UV and blue light, as depicted in Fig. 4.5. Similar emission

peaks have been observed around 592, 612, 655 and 703 nm [46]. The red emission peak at 612 nm related to the  $^5D_0 \rightarrow ^7F_2$  transition is the most intense among all the emission peaks.

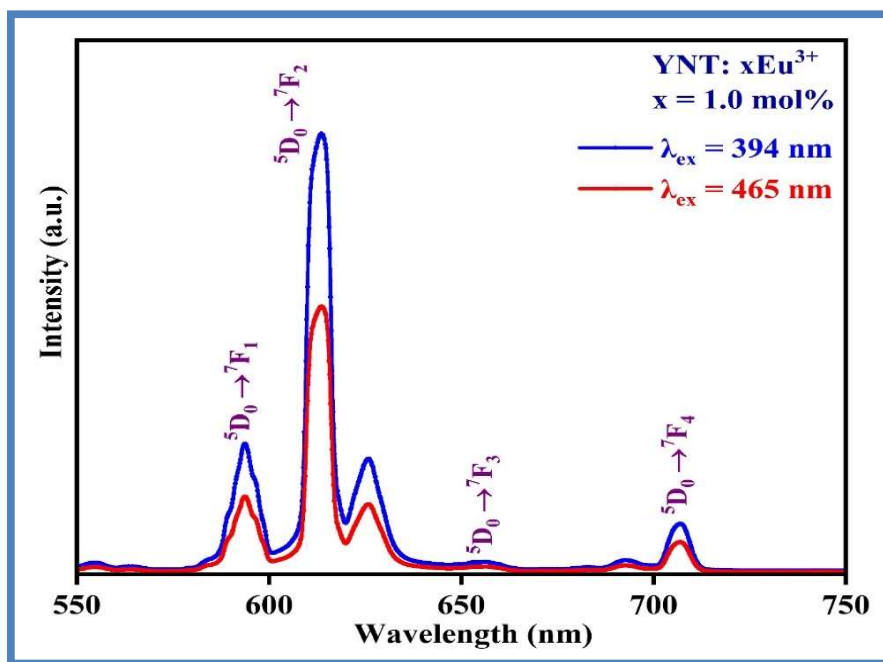


**Fig. 4.5. PL spectrum of YNT: 1.0 mol%  $Eu^{3+}$  phosphor under  $\lambda_{exc}= 394$  and 465 nm**

The intense  $^5D_0 \rightarrow ^7F_2$  transition is a forced electric dipole (ED) transition and complies with the selection rule ( $\Delta J = 2$ ), while the peak at 592 nm is associated with the  $^5D_0 \rightarrow ^7F_1$  transition is a magnetic dipole (MD) transition and obeys the selection ( $\Delta J = 1$ ) rule. The  $^5D_0 \rightarrow ^7F_1$  MD transition is independent of local symmetry around the dopant ions as well as their surroundings [49]. Conversely, the  $^5D_0 \rightarrow ^7F_2$  forced ED transition exhibits hypersensitivity and the intensity of this transition is significantly influenced by the crystal field of the ligand atoms [47, 49]. Moreover, the feeble peak around at 703 nm is attributed to the  $^5D_0 \rightarrow ^7F_4$  transition. A comparison of the emission intensity of synthesized YNT: 1.0 mol%  $Eu^{3+}$  phosphor along with different excitation wavelengths is demonstrated in Fig. 4.6.

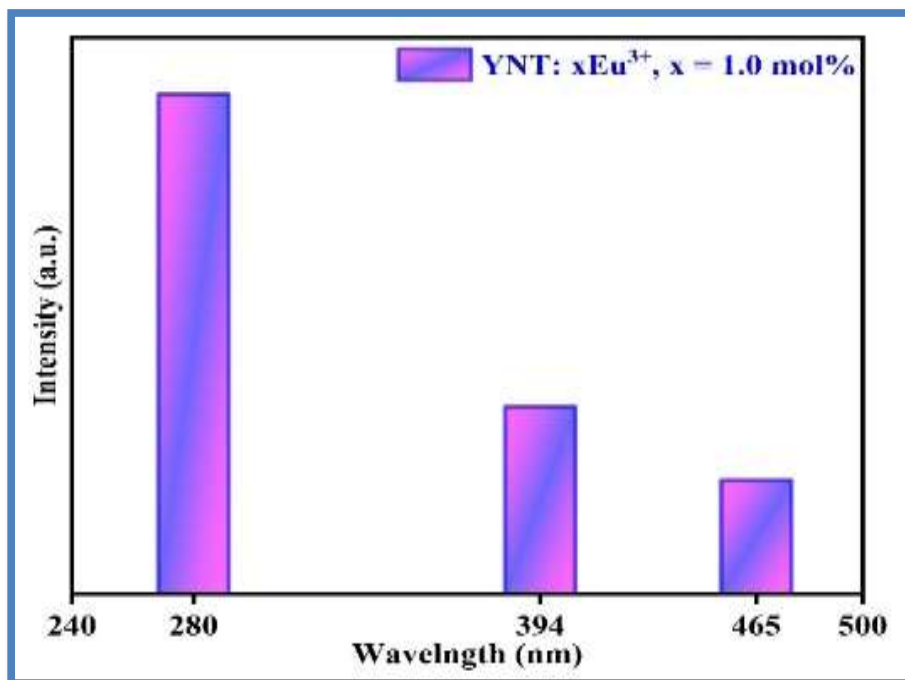


**Fig. 4.6. Comparison of emission intensity at different excitation wavelengths of the YNT: 1.0 mol% Eu<sup>3+</sup> phosphor**

It has been found that the emission intensity of synthesized phosphor is higher for UV light than for other n-UV and blue light excitations. Therefore, the synthesized YNT with 1.0 mol% Eu<sup>3+</sup> phosphor can effectively be excited with UV light for photonic applications.

#### **4.1.4. Colorimetric Studies**

The Commission International de l'Eclairage (CIE) ( $x, y$ ) coordinates have been computed using emission spectral data for the synthesized YNT: xEu<sup>3+</sup>, x = 1.0 mol% phosphor under UV, n-UV and blue light excitations. CIE coordinates for the synthesized YNT: 1.0 mol% Eu<sup>3+</sup> phosphor is presented in Fig. 4.7. The CIE ( $x, y$ ) coordinates are observed to be (0.406, 0.383) under UV light, which lies in the orange region of the chromaticity plot. Under the excitation of n-UV and blue lights, the CIE coordinates (0.632, 0.364) and (0.629, 0.366) are located in the red region of the CIE graph, which is adjacent to the commercial Y<sub>2</sub>O<sub>2</sub>S: Eu<sup>3+</sup> (0.647, 0.343) phosphor [47].

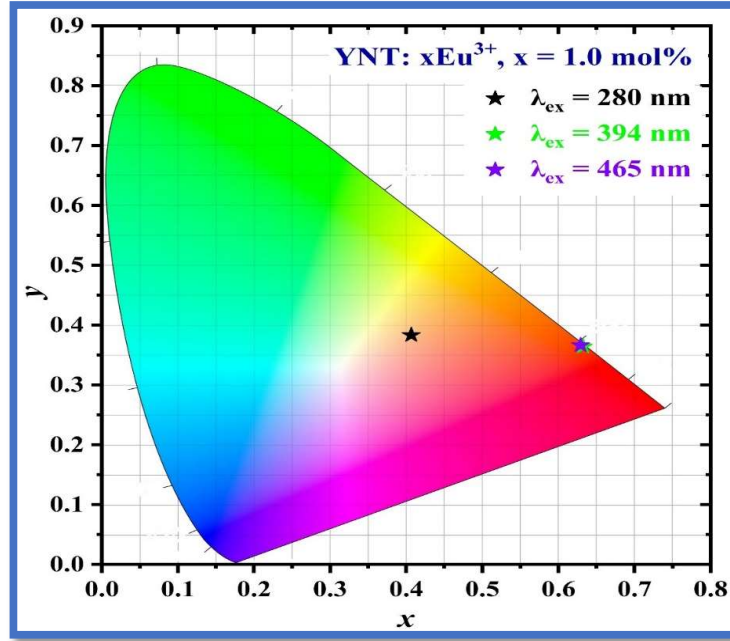


**Fig. 4.7. CIE chromaticity coordinates for the synthesized YNT: 1.0 mol% Eu<sup>3+</sup> phosphor under UV, n-UV and blue light.**

Moreover, the correlated colour temperature (CCT) values for the synthesized YNT: xEu<sup>3+</sup> phosphor have been determined with the help of McCamy's formula as given below [50, 51]:

$$CCT = -449.0 n^3 + 3525.0 n^2 - 6823.0 n + 5520.3 \quad (4.2)$$

in the above formula,  $n = \frac{x-x_e}{y-y_e}$ ;  $x_e = 0.332$  and  $y_e = 0.186$  are the epicentre, respectively.

The assessed value of CCT for the synthesized YNT doped with 1.0 mol% Eu<sup>3+</sup> phosphor has been observed to be 3420, 2090, and 2040 K under different excitation wavelengths of UV, n-UV and blue radiation, respectively. The samples with CCT values less than 5000 K are intended for warm light, whereas those above 5000 K are suitable for cool light applications. In the present investigation, the synthesized phosphor with lower CCT values (< 5000 K) is deemed suitable for the usage of photonic devices, especially for warm white LED applications.



## CHAPTER 5: CONCLUSIONS AND FUTURE SCOPE OF WORK

### 5.1. Conclusions

Single-phase yttrium niobium titanate phosphor ( $\text{YNbTiO}_6$ ) induced with trivalent europium ( $\text{Eu}^{3+}$ ) ions were successfully synthesized using a high-temperature SSR route and their structural, morphological and photoluminescent characteristics have been explored in detail. The diffraction profiles confirm that all peaks can be identified as the orthorhombic  $\text{YNbTiO}_6$  crystal structure. Also, it confirms that the  $\text{Eu}^{3+}$  ion inhabits the  $\text{Y}^{3+}$  site in the YNT host lattice lacking any changes to the orthorhombic structure. The agglomerated particles have been found to be in the micron range, as confirmed by FE-SEM analysis. Under the different UV, NUV and blue light, the emission spectral profile of the synthesized YNT: 1.0 mol%  $\text{Eu}^{3+}$  phosphor revealed several characteristic peaks and the most intense peak was observed around the red (612 nm) region. CIE coordinates (0.406, 0.383) are located in the orange region under UV light, whereas under NUV and blue light, the color coordinates (0.632, 0.364) and (0.629, 0.366) are located in the red region of the CIE graph. Moreover, the CCT values of the synthesized phosphor were found to be 3420, 2090, and 2040 K under different excitation wavelengths. Henceforth, the result mentioned above confirms that the synthesized YNT induced  $\text{Eu}^{3+}$  ions can be beneficial for the usage of photonic application.

## 5.2. Future Scope of Work

The present work has been done by developing red emitting YNT: Eu<sup>3+</sup> phosphor as a cost effective, low energy consumption and environmental-friendly red component in pc w-LEDs. In order to improve the photoluminescent properties of the proposed luminescent material, doping concentration of Eu<sup>3+</sup> (activator ions) can be increased until concentration quenching occurs. By that we can achieve the optimum dopant concentration for maximum photoluminescent intensity. Further, color tunable characteristics of phosphor material can be attained by co-doping rare earth ions such as erbium (Er<sup>3+</sup>), dysprosium (Dy<sup>3+</sup>), samarium (Sm<sup>3+</sup>), etc into the host matrix.

The present phosphor material has been synthesized by using high temperature solid state reaction method and characterized at room temperature for probing its structural and luminescent properties. Hence, another synthesis route such as sol-gel method can also be explored to improve the particles' morphology. Moreover, characterization techniques like time resolved photoluminescence (TRPL) spectroscopy and temperature dependent photoluminescence (TDPL) spectroscopy can be utilized to measure the lifetime of excited states and thermal stability of luminescent materials, respectively.

Usefulness of prepared phosphor material is not just limited to application in w-LED but can be extended for other applications such as fingerprint sensing, bio-imaging, etc. In summary, as synthesized red emitting YNT: Eu<sup>3+</sup> phosphor material can be used as an effective component for photonic applications.

## **REFERENCES**

- [1] H.S. Virk, Defect and Diffusion Forum 361 1-13 (2015)
- [2] K.V.R. Murthy, Int. J. Lumin. Appl 302-315 (2015)
- [3] S. Kaur, PhD diss., Delhi Technological University (2019)
- [4] M.K. Sahu, PhD diss., Delhi Technological University (2023)
- [5] Y. Lin, D. He, K. Jiang, R. Qin, J. Wang, Y. Shao, J. Yan, R. Yu, D. Zhang, S. Xie, L. Zhao, J. Alloys Compd. 960 170563 (2023)
- [6] Deepali, PhD diss., Delhi Technological University (2023).
- [7] H. Kaur, PhD diss., Delhi Technological University (2021).
- [8] S.K. Gupta, R. M. Kadam, P. K. Pujari, Coord. Chem. Rev 420 213405 (2020)
- [9] I. Gupta, Isha, S. Singh, S. Bhagwan, D. Singh, Ceram. Int. 47(14) 19282-19303 (2021)
- [10] D. Nagpal, T. Bhadauria, M. Jayasimhadri, Mater. Today Proc. 62 3719-3723 (2022)
- [11] S. Kaur, M. Jayasimhadri, A. S. Rao, J. Alloys Compd. 697 367-373 (2017)
- [12] Y. Shi, R. Cui, X. Liu, J. Hu, P. Yu, J. Zhang, C. Deng, J. Solid State Chem. 323 124039. (2023)
- [13] S.Ye, F. Xiao, Y. X. Pan, Y. Y. Ma, Q. Y. Zhang, Mater. Sci. Eng. 71 1-34 (2010)
- [14] M. Rajendran, S. Vaidyanathan, ChemistrySelect 5(17) 5128-5136 (2020)
- [15] G.B. Nair, H. C. Swart, S. J. Dhoble, Prog. Mater. Sci. 109 100622 (2020)
- [16] V. Sangwan, M. Jayasimhadri, D. Haranath, J. Lumin. 266 120276 (2024)


- [17] S. Kaur, M. Jayasimhadri, A. S. Rao, *J. Alloys Compd.* 697 367-373 (2017)
- [18] Q. Ma, M. Lu, P. Yang, A. Zhang, Y. Cao *Mater. Res. Bull.* 48(10) 3677-3686 (2013)
- [19] M.L. Meena, S. Som, C.H. Lu, R.S. Badgoti, S. Dutta, R.K. Singh, S.D. Lin, H. C. Swart,  
In *Metal Oxide-Based Heterostructures* 297-330 (2023)
- [20] A. Buekenhoudt, A. Kovalevsky, J. Luyten, F. Snijkers, *Comprehensive Membrane  
Science and Engineering*; Drioli, E., Giorno, L., Eds 217-252 (2010)
- [21] S. Ivanov, In *Science and Technology of Atomic, Molecular, Condensed Matter &  
Biological Systems 2* 163-238 (2012)
- [22] V. Kumar, S. P. Tiwari, O. M. Ntwaeaborwa, Hendrik C. Swart, In *Spectroscopy of  
Lanthanide Doped Oxide Materials*, Woodhead Publishing 345-364 (2020)
- [23] H. Sun, W. Wei, F. Liu, X. Xu, Z. Li, Z. Liu, *J. Alloys Compd.* 972 172839 (2024)
- [24] D. Bokov, A.T. Jalil, S. Chupradit, W. Suksatan, M.J. Ansari, I.H. Shewael, G.H. Valiev,  
E. Kianfar *MSEJ* 1-21 (2021)
- [25] E. Yilmaz, M. Soylak, In *Handbook of Nanomaterials in analytical chemistry* 375-413  
(2020)
- [26] L. Baraket, A. Ghorbel, In *Studies in surface science and catalysis* 118 657-667 (1998)
- [27] S. Sakka, Sumio, *Handbook of sol-gel science and technology. vol. 3.* Springer Science  
& Business Media 3-105 (2005)
- [28] D. O'hare, D, *Encyclopedia of Materials: science and Technology* 3989-3992 (2001)
- [29] E.B. Denkbas, E. Celik, E. Erdal, D. Kavaz, Ö. Akbal, G. Kara, C. Bayram,  
In *Nanobiomaterials in Drug Delivery*, William Andrew Publishing 285-331 (2016)

- [30] B.P. Kafle, Chemical analysis and material characterization by spectrophotometry 6 147-198 (2020)
- [31] S.K. Gupta, Y. Mao, J. Phys. Chem. C 125(12) 6508-6533 (2021)
- [32] S.K. Gupta, Y. Mao, Prog. Mater. Sci. 117 100734 (2021)
- [33] N.S. Bajaj, R. A. Joshi, Energy Mater. 61-82 (2021)
- [34] F. Wang, X. Liu, Compr Nanosci Nanotechnol 2019 359 (2019)
- [35] C. Li, M. Li, A.C. Veen, In Advanced Nanomaterials for Catalysis and Energy 1-28 (2019)
- [36] Z. Yu, G. Zhou, J. Zhou, H. Zhou, P. Kong, Y. Wu, H. Huang, X. Yu, X. Zhang, R. Zhang, RSC Adv. 5(115) 94607-94614 (2015)
- [37] Q. Ma, Y. Zhou, A. Zhang, M. Lu, G. Zhou, C. Li, Solid State Sci. 11(6) 1124-1130 (2009)
- [38] Y. Shi, Y. Wang, Z. Yang, J. Alloys Compd. 509(6) 3128-3131 (2011)
- [39] P. Sharma, M. Kaushik, M. Jayasimhadri, Defect and Diffusion Forum, 430 71-78 (2024)
- [40] R.P. Jaya, New Materials in Civil Engineering 493-527 (2020)
- [41] A. Mayeen, L.K. Shaji, A.K. Nair, & N. Kalarikkal, CAN., Woodhead Publishing 335-364 (2018)
- [42] H. Pei, L.M. Su, G.M. Cai, Z.P. Jin, AIP Adv. 8 045107 (2018)
- [43] M.K. Sahu, M. Jayasimhadri, J. Lumin. 277 117570 (2020)
- [44] L. Alexander, H.P. Klug, J. Appl. Phys. 21 137-142 (1950)
- [45] H. Kaur, M. Jayasimhadri, Ceram. Int. 45 15385-15393 (2019)

- [46] A.K. Parchur, R.S. Ningthoujam, *RCS Adv.* 2 10859-10868 (2017)
- [47] Vikas, M. Jayasimhadri, D. Haranath, *Curr. Appl. Phys.* 58 11-20 (2024)
- [48] W.T. Carnall, P.R. Fields, K. Rajnak, *J. Chem. Phys.* 49 4450-4455 (1968)
- [49] T. A. Jose, J. R. Jose, A. Gopinath, M. S. Amogh, C. Joseph, P. R. Biju, *Mater. Res. Bull.* 174 112699 (2024)
- [50] C.S. McCamy, *Color Res. Appl.* 17 142-144 (1992)
- [51] V. Sangwan, M. Jayasimhadri, D. Haranath, *J. Phys. D: Appl. Phys.* 57(19) 195301 (2024)

## CONFERENCE PROOF

### I. CONFERENCE ACCEPTANCE PROOF

2K22MSCPHY47 VEDIKA <vedika\_2k22mscphy47@dtu.ac.in>

---

**Acceptance Letter for 2nd International Conference on Recent Advances in Functional Materials (RAFM-2024)**

rafm@arsd.du.ac.in <rafm@arsd.du.ac.in>  
To: vedika\_2k22mscphy47@dtu.ac.in

**ACCEPTANCE LETTER**

Dear Ms. VEDIKA DUBEY  
**DELHI TECHNOLOGICAL UNIVERSITY**  
Greetings!!

ARSD College welcomes you to the 2nd International conference on Recent Advances in Functional Materials (RAFM-2024).

RAFM-2024 to be held online mode at Atma Ram Santan Dharma College, University of Delhi during March 14-16, 2024, which is being organized by Department of Physics, IQAC and matter of great pleasure that the technical committee accepted your research paper entitled:

**Luminescent features of red emitting Eu<sup>3+</sup> induced yttrium niobium titanate phosphor for photonic applications**


You are invited for a presentation of the same at RAFM-2024 as **Oral Presentation**.

Time allotted for oral presentation is **10 (8+2) Min**, and the participant is requested to report and present online your paper within stipulated time.

Please confirm participation through registration fees in favor of **Atma Ram Santan Dharma College** (ignore if already paid). The details of registration are on <http://conference.arsdcollege.ac.in/rafm2024>. Only registration fee paid abstracts will be published in the Abstract book. **Best Oral / Poster presentation certificates will be** in conference and accepted after review through due process, will be published **without any fee** in the Scopus indexed and peer reviewed journals as per the policy of the journals:

- Springer Nature (SCOPUS)
- IONICS, Springer (SCOPUS)
- Current Natural Science & Engineering, VVBF

### II. PUBLICATION ACCEPTANCE PROOF

2K22MSCPHY47 VEDIKA <vedika\_2k22mscphy47@dtu.ac.in>

---

**Fwd: Decision Letter (RAFM\_11)**

Dr. Jayasimhadri M <jayasimha@dtu.ac.in> Wed, Jun 5, 2024 at 9:37 PM  
To: 2K22MSCPHY47 VEDIKA <vedika\_2k22mscphy47@dtu.ac.in>

----- Forwarded message -----  
From: **RAFM-2024, Department of Physics ARSD College** <rafm@arsd.du.ac.in>  
Date: Wed, 5 Jun 2024, 21:07  
Subject: Decision Letter (RAFM\_11)  
To: <jayasimha@dtu.ac.in>  
Cc: Subhash Sharma <subhash1jiit@gmail.com>

Ms. Ref. No.: RAFM\_11  
Title: Luminescent features of red emitting Eu<sup>3+</sup> induced yttrium niobium titanate phosphor for photonic applications

Dear Dr. M. Jayasimhadri

I am pleased to inform you that your paper "Luminescent features of red emitting Eu<sup>3+</sup> induced yttrium niobium titanate phosphor for photonic applications" **Select Springer Nature Proceedings of RAFM 2024 (Scopus Indexed)**".

**Regards**  
Editor, RAFM-2024

### III. PROOF OF SCOPUS INDEXING

6/1/24, 4:58 PM Publication





**2nd International Conference on  
RECENT ADVANCES IN FUNCTIONAL MATERIALS  
(RAFM-2024)**  
**14-16 March 2024**

**Organized by:**  
Department of Physics & IQAC, Atmā Ram Sanatan Dharma College, (University of Delhi)  
Dhaura Kuan, New Delhi, INDIA-110021

## PUBLICATION

Research papers presented in the conference and accepted after review through due process will be published in the Scopus indexed and peer-reviewed journals.



- Springer Nature (SCOPUS)
- IONICS, Springer (SCOPUS)



- Current Natural Science & Engineering, VVBF



# PLAGIARISM REPORT

**Similarity Report**

---

<b>PAPER NAME</b> <b>Msc Report_1 - Copy.docx</b>	<b>AUTHOR</b> <b>Vedika Dubey</b>
------------------------------------------------------	--------------------------------------

---

<b>WORD COUNT</b> <b>6431 Words</b>	<b>CHARACTER COUNT</b> <b>36098 Characters</b>
<b>PAGE COUNT</b> <b>34 Pages</b>	<b>FILE SIZE</b> <b>2.8MB</b>
<b>SUBMISSION DATE</b> <b>Jun 3, 2024 4:22 PM GMT+5:30</b>	<b>REPORT DATE</b> <b>Jun 3, 2024 4:23 PM GMT+5:30</b>

---

- **9% Overall Similarity**  
The combined total of all matches, including overlapping sources, for each database.
  - 4% Internet database
  - Crossref database
  - 6% Submitted Works database
  - 6% Publications database
  - Crossref Posted Content database
  
- **Excluded from Similarity Report**
  - Small Matches (Less than 10 words)